

Supporting Information

Clarifying the controversial catalytic active sites of Co_3O_4 for oxygen evolution reaction

Yong Xu,^a Fengchu Zhang,^b Tian Sheng,^c Tao Ye,^b Ding Yi,^b Yijun Yang,^b Shoujie Liu,^c Xi

Wang^{b,*} and Jiannian Yao^{a, c, d,*}

^a School of Chemical Engineering and Technology, Tianjin University; Institute of Molecular Plus, Tianjin University, Tianjin, 300072, P. R. China

E-mail: jnyao@iccas.ac.cn

^b Key Laboratory of Luminescence and Optical Information, Ministry of Education, Department of Physics, School of Science, Beijing Jiaotong University, Beijing, 100044, P. R. China

E-mail: xiwang@bjtu.edu.cn

^c Chemistry and Chemical Engineering Guangdong Laboratory Shantou 515031, P. R. China

^d Key Laboratory of Photochemistry, Institute of Chemistry, Chinese Academy of Sciences, Beijing, 100190, China

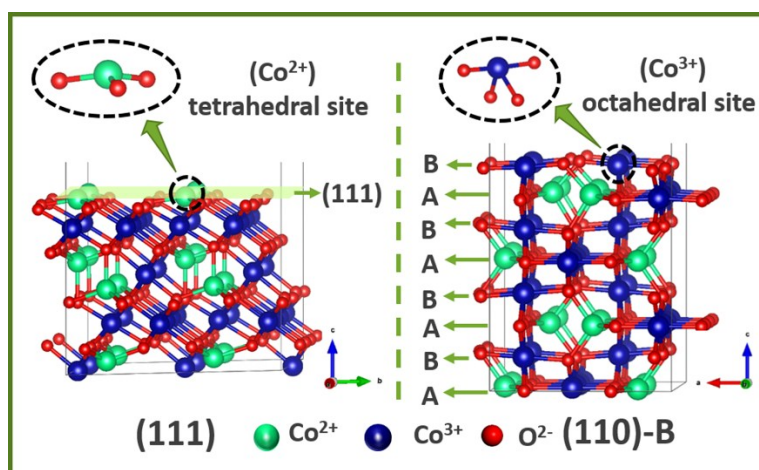


Fig. S1 The side-view of Co_3O_4 structure and the surface atomic configurations in the (111) plane (right) and the (110)-B plane (left).

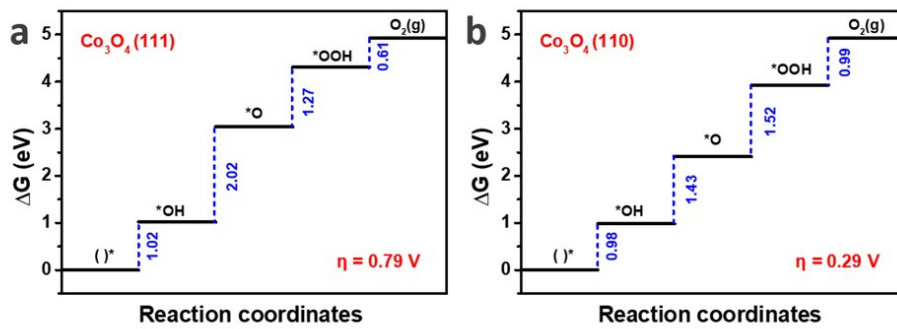


Fig. S2 The calculated OER free energy diagram over the (111) plane (a) and (110)-B plane (b) of Co_3O_4 . Free energy diagram for Co_3O_4 (111) and Co_3O_4 (110)-B for OER at zero potential ($U = 0$).

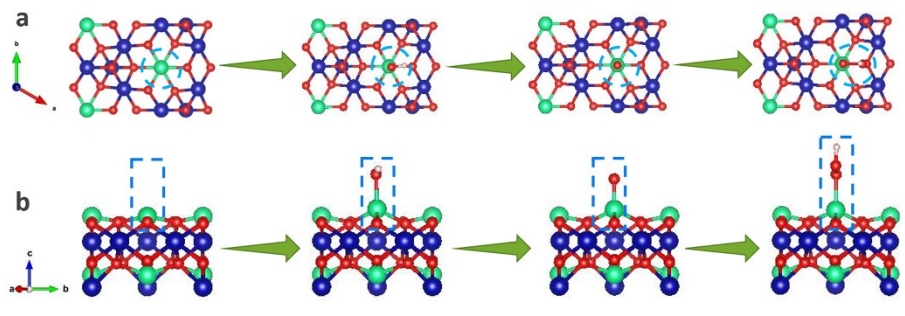


Fig. S3 Adsorption configurations over the (111) plane of Co_3O_4 , (a) top-view and (b) side-view.

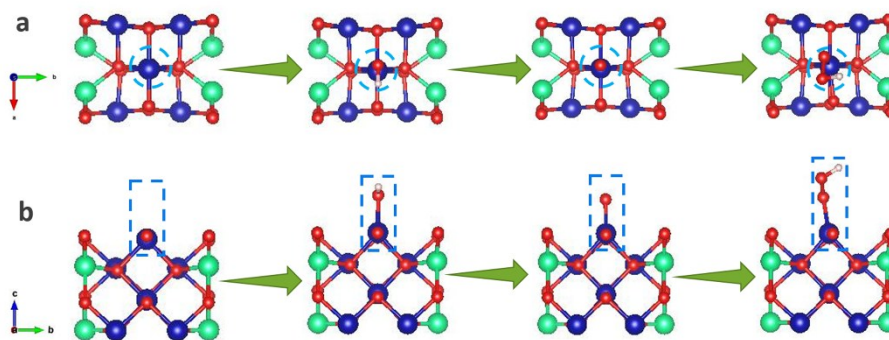


Fig. S4 Adsorption configurations over the (110)-B plane of Co_3O_4 , (a) top-view and (b) side-view.

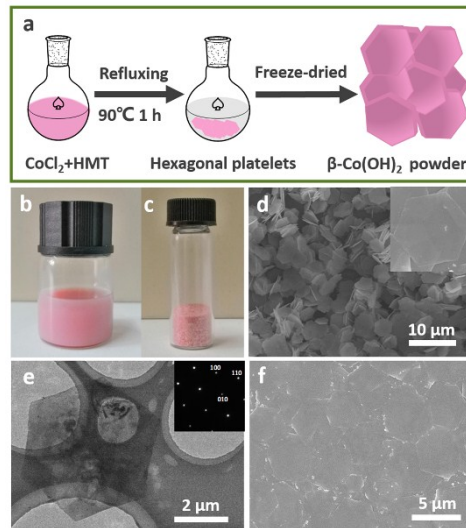


Fig. S5 (a) Schematic illustration of the synthesis for hexagonal platelets of $\beta\text{-Co(OH)}_2\text{-5.0}$. (b) The suspension of $\beta\text{-Co(OH)}_2\text{-5.0}$ in ethanol. (c) The powder of the $\beta\text{-Co(OH)}_2\text{-5.0}$ hexagonal platelets made by freeze-dried. (d) SEM images of $\beta\text{-Co(OH)}_2\text{-5.0}$ hexagonal platelets at low and high magnification (Inset). (e) TEM image of $\beta\text{-Co(OH)}_2\text{-5.0}$ hexagonal platelet and typical electron diffraction pattern (Inset). (f) SEM image of $\beta\text{-Co(OH)}_2\text{-5.0}$ film fabricated by the hexane/water interfacial self-assembly strategy.

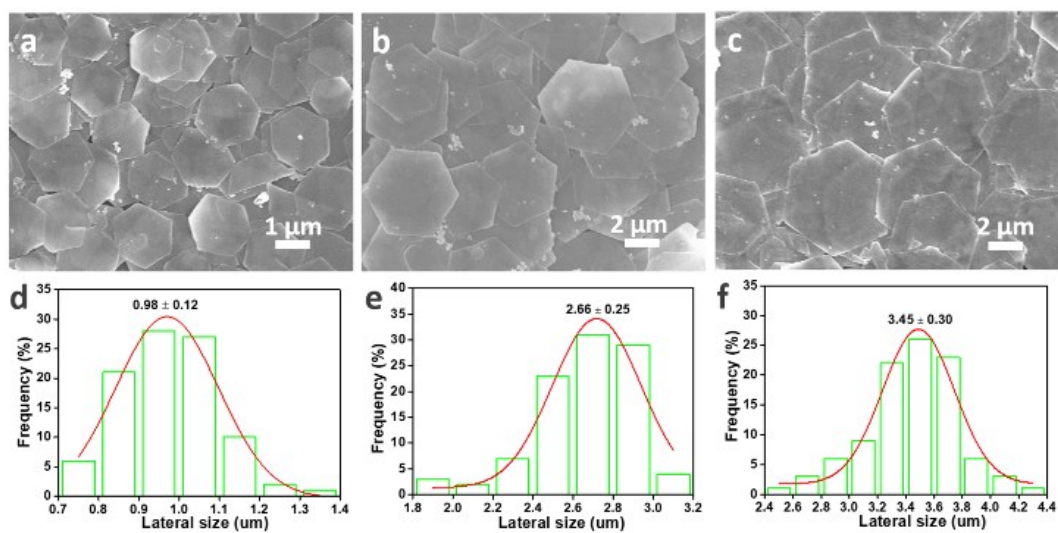


Fig. S6 (a-c) The SEM images of $\beta\text{-Co(OH)}_2\text{-2.5}$, $\beta\text{-Co(OH)}_2\text{-5.0}$ and $\beta\text{-Co(OH)}_2\text{-7.5}$, respectively. (d-f) The corresponding lateral size distributions of $\beta\text{-Co(OH)}_2\text{-2.5}$, $\beta\text{-Co(OH)}_2\text{-5.0}$ and $\beta\text{-Co(OH)}_2\text{-7.5}$.

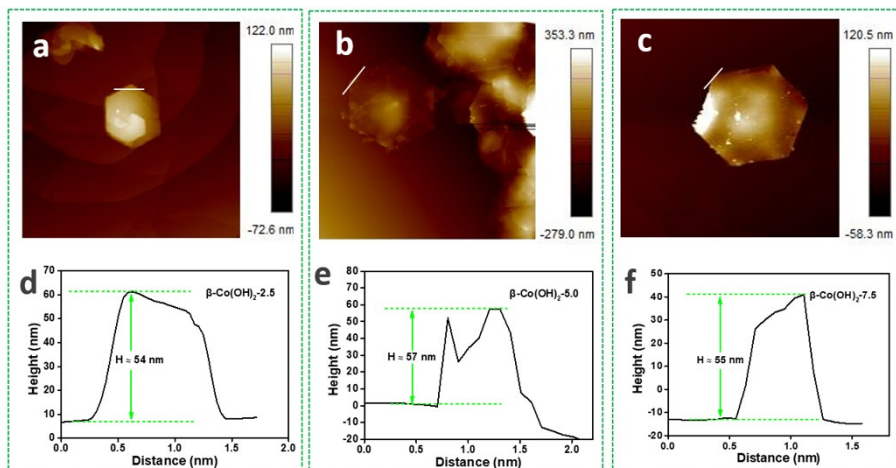


Fig. S7 AFM images of (a) $\beta\text{-Co(OH)}_2\text{-2.5}$, (b) $\beta\text{-Co(OH)}_2\text{-5.0}$ and (c) $\beta\text{-Co(OH)}_2\text{-7.5}$. The corresponding thickness measurement data of (d) $\beta\text{-Co(OH)}_2\text{-2.5}$, (e) $\beta\text{-Co(OH)}_2\text{-5.0}$ and (f) $\beta\text{-Co(OH)}_2\text{-7.5}$.

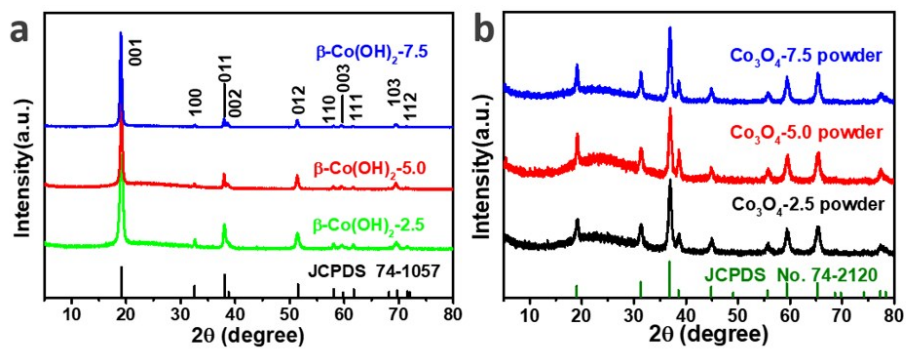


Fig. S8 (a) XRD pattern of synthesized pink powder of $\beta\text{-Co(OH)}_2\text{-2.5}$, $\beta\text{-Co(OH)}_2\text{-5.0}$ and $\beta\text{-Co(OH)}_2\text{-7.5}$. (b) XRD patterns of $\text{Co}_3\text{O}_4\text{-2.5}$, $\text{Co}_3\text{O}_4\text{-5.0}$ and $\text{Co}_3\text{O}_4\text{-7.5}$.

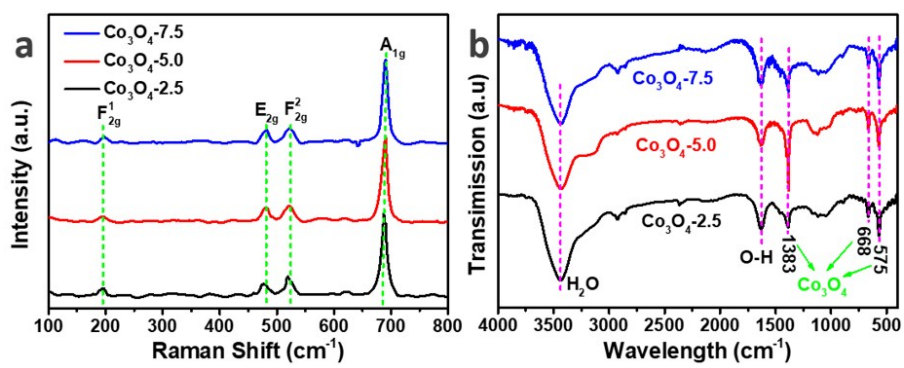


Fig. S9 (a) Raman spectra of synthesized Co_3O_4 -2.5, Co_3O_4 -5.0, and Co_3O_4 -7.5 powder. (b) FTIR spectra of synthesized Co_3O_4 -2.5, Co_3O_4 -5.0, and Co_3O_4 -7.5 powder.

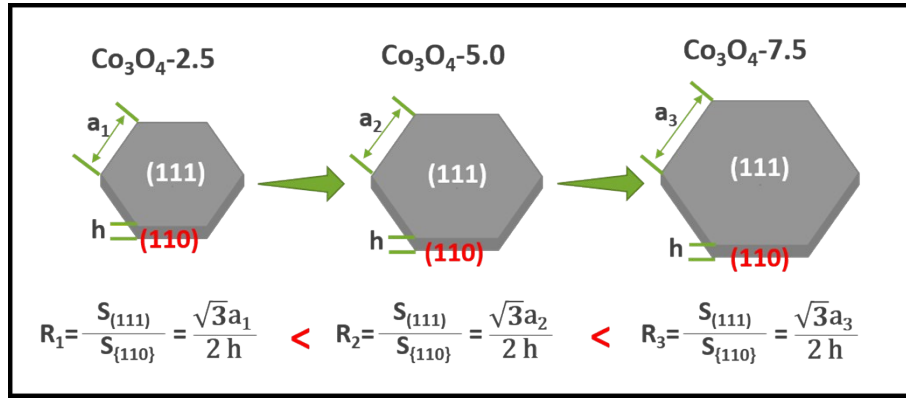


Fig. S10 Structure models of $\text{Co}_3\text{O}_4\text{-2.5}$, $\text{Co}_3\text{O}_4\text{-5.0}$ and $\text{Co}_3\text{O}_4\text{-7.5}$ hexagonal platelets and the corresponding ratios (R_1 - R_3) of the (111) planes and {110} planes.

($S_{(111)}$: the area of both top and bottom regular hexagons ((111) planes); $S_{\{110\}}$: the area of six side rectangles ({110} planes). a_1 - a_3 : the lateral sizes of $\text{Co}_3\text{O}_4\text{-2.5}$, $\text{Co}_3\text{O}_4\text{-5.0}$ and $\text{Co}_3\text{O}_4\text{-7.5}$, respectively. h : the thickness of the $\text{Co}_3\text{O}_4\text{-2.5}$, $\text{Co}_3\text{O}_4\text{-5.0}$ and $\text{Co}_3\text{O}_4\text{-7.5}$. $R_1 : R_2 : R_3 = a_1 : a_2 : a_3 = 1.0 : 2.7 : 3.5$.)

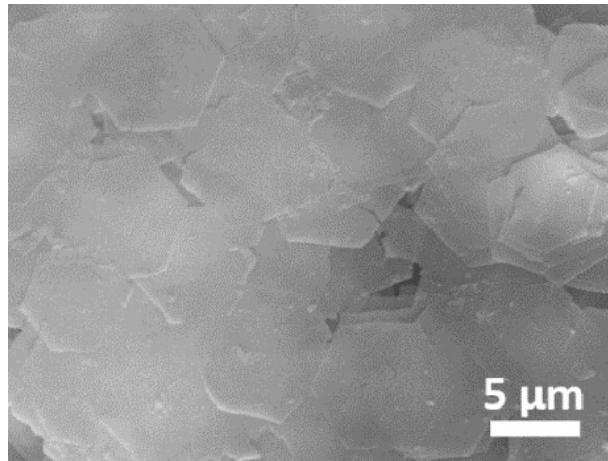


Fig. S11 The SEM images of Co_3O_4 -5.0 hexagonal platelets on the surface of conductive silicon substrate.

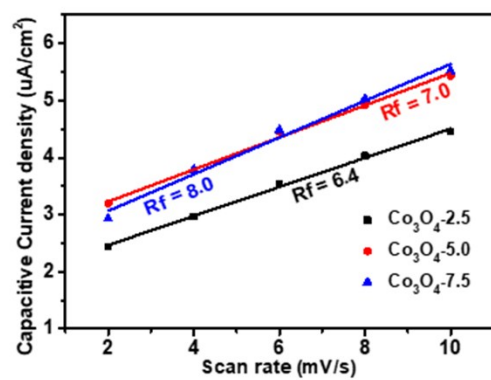


Fig. S12 Dependence relation of the capacitive current vs. scan rate for Co₃O₄-2.5, Co₃O₄-5.0 and Co₃O₄-7.5.

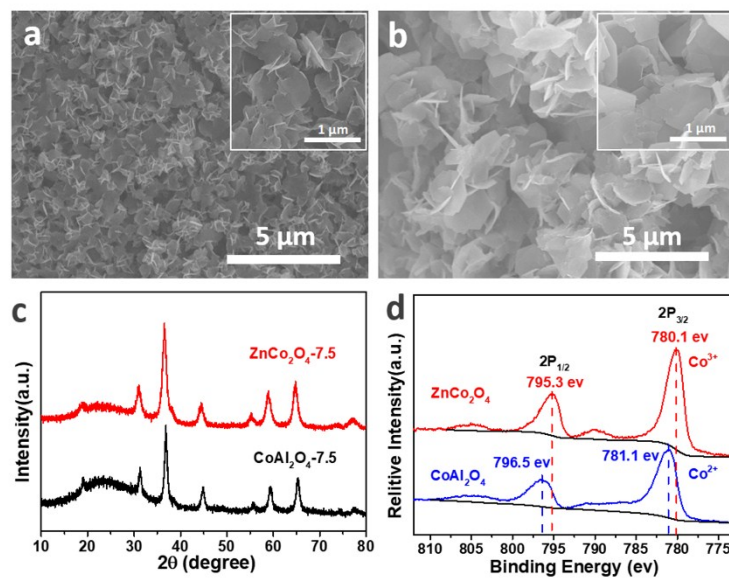


Fig. S13 (a, b) SEM images of CoAl₂O₄-7.5 and ZnCo₂O₄-7.5 at low and high (inset) magnification, respectively. (c) XRD pattern of CoAl₂O₄-7.5 and ZnCo₂O₄-7.5. (d) XPS spectra of the Co 2p in CoAl₂O₄-7.5 and ZnCo₂O₄-7.5.

(The CoAl₂O₄-7.5 and ZnCo₂O₄-7.5 were synthesised with the same method as Co₃O₄-7.5. In synthesis procedure of the precursor, the amounts of CoCl₂·6H₂O with AlCl₃ (Co/Al = 1/2) and CoCl₂·6H₂O with ZnCl₂ (Co/Zn = 2/1) were dissolved to give the total concentrations of 7.5 mM, respectively. The samples were denoted as CoAl₂O₄-7.5 and ZnCo₂O₄-7.5, respectively.)

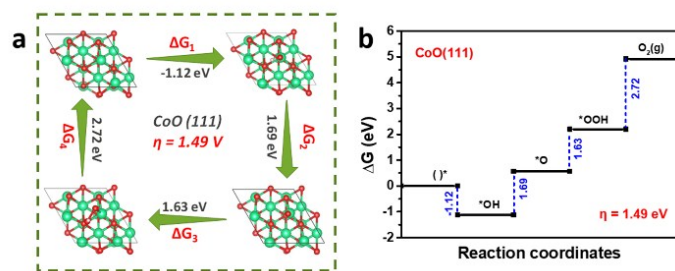


Fig. S14 (a) Adsorption configurations over the (111) plane of CoO. (b) The calculated OER free energy diagram over the (111) plane of CoO.